scientific reports

Check for updates

OPEN

Quantitative comparison of automated OCT and conventional FAF-based geographic atrophy measurements in the phase 3 OAKS/DERBY trials

Julia Mai[1], Gregor S. Reiter[1], Sophie Riedl[1], Wolf-Dieter Vogl[2], Amir Sadeghipour[2], Emma Foos[3], Alex McKeown[3], Hrvoje Bogunovic[1] & Ursula Schmidt-Erfurth[1]✉

With the approval of the first two substances for the treatment of geographic atrophy (GA) secondary to age-related macular degeneration (AMD), a standardized monitoring of patients treated with complement inhibitors in clinical practice is needed. Optical coherence tomography (OCT) provides high-resolution access to the retinal pigment epithelium (RPE) and neurosensory layers, such as the ellipsoid zone (EZ), which further enhances the understanding of disease progression and therapeutic effects in GA compared to conventional fundus autofluorescence (FAF). In addition, artificial intelligence-based methodology allows the identification and quantification of GA-related pathology on OCT in an objective and standardized manner. The purpose of this study was to comprehensively evaluate automated OCT monitoring for GA compared to reading center-based manual FAF measurements in the largest successful phase 3 clinical trial data of complement inhibitor therapy to date. Automated OCT analysis of RPE loss showed a high and consistent correlation to manual GA measurements on conventional FAF. EZ loss on OCT was generally larger than areas of RPE loss, supporting the hypothesis that EZ loss exceeds underlying RPE loss as a fundamental pathophysiology in GA progression. Automated OCT analysis is well suited to monitor disease progression in GA patients treated in clinical practice and clinical trials.

Keywords Geographic atrophy, Optical coherence tomography, Fundus autofluorescence, Artificial intelligence, Deep learning

The first treatment for geographic atrophy (GA) secondary to age-related macular degeneration (AMD), namely pegcetacoplan (Syfovre), has been approved at the beginning of 2023 by the Food and Drug Administration (FDA)[1]. Pegcetacoplan is a complement C3-inhibitor administered as intravitreal injection, which significantly reduced the GA lesion growth in treated patients versus untreated patients in the phase 2 FILLY trial as well as in the phase 3 OAKS and DERBY trials[2,3]. Subsequently, avacincaptad pegol (Izervay), a complement C5-inhibitor, has been approved by the FDA for the treatment of GA secondary to AMD later that year[4,5].

In the trials, fundus autofluorescence (FAF) was used as an imaging modality to measure GA lesion growth over time as the primary endpoint. As a 2D imaging modality, blue-light (488 nm) FAF can be used to assess the integrity of the retinal pigment epithelium (RPE) and its loss is quantified as sharply demarcated hypofluorescent areas[6]. It detects the autofluorescence of fluorophores, mainly lipofuscin from visual cycle by-products, which accumulates within RPE cells[7]. However, it is known that GA not only affects the RPE but also the neurosensory layers like the photoreceptors (PR), as it is a progressive neurodegenerative disease. Consequently, the suitability of 2D FAF for disease imaging and monitoring of multiple retinal layers is limited[8].

This work was in parts presented at the Annual Meeting of the Association of Research in Vision and Ophthalmology 2023.

[1]OPTIMA - Laboratory for Ophthalmic Image Analysis, Department of Ophthalmology and Optometry, Medical University of Vienna, Vienna, Austria. [2]RetInSight, Vienna, Austria. [3]Apellis Pharmaceuticals, Waltham, MA, USA. ✉email: ursula.schmidt-erfurth@meduniwien.ac.at

The different retinal layers can be visualized in vivo with optical coherence tomography (OCT) by providing high resolution 3D images of the macula[9]. OCT is already used as the gold standard to monitor patients with neovascular AMD (nAMD) receiving anti-VEGF treatment and offers a better patient comfort than blue-light FAF[10]. Moreover, the clinically highly relevant assessment of foveal involvement in GA patients is more reliable on OCT than on blue-light FAF, because the fovea physiologically appears hypofluorescent due to absorption of the blue light[11]. In summary, OCT offers several advantages and more detailed information about the disease extent in GA compared to FAF, making it more suitable for monitoring the disease activity and progression in GA patients in the clinical setting, especially under therapeutic conditions.

In the clinical trials of pegcetacoplan, the measurement of the GA lesion growth on FAF was done manually by a centralized reading center. As the drug has now entered clinical routine, this is not a practical approach to handle the large amount of patients needing regular follow-up visits. Automated image analysis by means of artificial intelligence (AI), especially deep learning (DL), can be used to automatically delineate retinal layers and quantify pathologic features on OCT[12]. By evaluating the condition of PR layers, defined as ellipsoid zone (EZ) loss in our analysis, in addition to the RPE, automated OCT analysis can be used to assess the growth rate, offer therapeutic guidance and quantify the therapeutic effect in GA patients in a fast and objective way[13,14]. However, the correlation between the manual FAF measurements from clinical trials and automated OCT measurements still needs to be investigated for clinical application and to offer standardized monitoring of GA patients receiving regular treatment.

In this work, we comprehensively evaluated the correlation between reading center-based manual FAF measurements and automated OCT measurements for reliable assessment of RPE loss and EZ loss of GA lesions in the phase 3 OAKS and DERBY trials.

Methods

Study design and participants

This study is a post-hoc analysis of the prospective, multicenter, randomized, sham-controlled phase 3 OAKS (NCT03525613, first submitted 20/04/2018) and DERBY (NCT03525600, first submitted 20/04/2018) trials[3]. The trials investigated intravitreal pegcetacoplan, a complement C3 inhibitor, for the treatment of GA secondary to AMD. Patients enrolled in the trials had to be at least 60 years of age with a diagnosis of GA secondary to AMD based on FAF imaging. Further major criteria for inclusion were best corrected visual acuity (BCVA) of 24 letters or better using Early Treatment Diabetic Retinopathy Study (ETDRS) charts (20/320 Snellen equivalent), GA area size measured on FAF between 2.5 mm^2 and 17.5 mm^2, presence of any pattern of hyperautofluorescence in the junctional zone of GA, and in case of multifocal GA at least one focal lesion of 1.25 mm^2 or more. Subfoveal as well as non-subfoveal GA lesions were included. Patients were excluded if the study eye showed GA secondary to other causes than AMD, history or current evidence of exudative AMD, and retinal disease other than AMD.

Patients were randomized in a 2:2:1:1 manner to receive 15 mg intravitreal pegcetacoplan monthly (PM), every other month (PEOM) and sham injections monthly (SM) or every other month (SEOM). The primary end point was the GA lesion growth over 12 months, measured manually on FAF by a centralized reading center. Patients were imaged every two months up to month 24 with FAF as well as SD-OCT[3].

All patients provided written informed consent. The study was performed in accordance with the tenets of the Declaration of Helsinki and the International Conference on Harmonization Good Clinical Practice guidelines. This post-hoc analysis was approved by the ethics committee at the Medical University of Vienna (EK Nr: 1246/2016).

Image analysis

Patients imaged using a Spectralis HRA + OCT device (Heidelberg Engineering, Heidelberg, Germany) were included in this post-hoc analysis. FAF images were acquired using blue light with an excitation at 488 nm and with a frame size of 30 × 30 degrees with a resolution of 768 × 768 pixels. SD-OCT volumes were acquired as volumes of 49 B-Scans of each 512 A-scans, with a pixel area of approximately 120 × 11.25 μm^2, covering the central 20 degrees of the macula. The optical axial resolution of the standard Spectralis device is 7 µm and the digital axial resolution is 3.9 µm/pixel. The OCT volumes were registered using the follow-up mode of the device. FAF images were manually delineated by an independent centralized reading center (Digital Angiography Reading Center, Great Neck, NY), where GA was defined as sharply demarcated hypofluorescent area. The OCT images were analyzed in a fully automated way by two previously developed and validated deep learning-based algorithms for the segmentation of RPE loss and EZ loss[15,16]. The algorithms have been extensively validated and achieve a precision that does not require manual corrections[13,17]. Both algorithms use fully convolutional neural networks (CNN) with enhanced U-shaped structures to obtain pixel-accurate segmentation of the targeted structures. The algorithm for the RPE loss segmentation is based on a 3D-to-2D CNN that segments the whole 3D-OCT volume as a 2D-en face map reflecting the location and size of the clinical appearance of the GA lesion. By taking the whole 3D volume as input, the algorithm benefits from the full volumetric context[15].

The algorithm for the EZ loss segmentation is based on an ensemble of 4 different U-shaped CNNs, leading to a more accurate segmentation than with a single-network approach. The algorithm segments the area between the top of the EZ and the outer boundary of the interdigitation zone (i.e., the third hyperreflective outer retinal band)[16]. For each single A-scan, a thickness value is provided and an en face PR thickness map can be calculated. In a postprocessing step, EZ loss was defined as an axial EZ thickness of ≤ 4 µm, which corresponds to the thickness that is visible as a single pixel on the image. The algorithms delineate the RPE and EZ layers on each individual B-scan of the entire OCT volume. The en face maps of the RPE loss and EZ loss segmentation can directly be brought in registration. Example images of manual en face RPE loss segmentation on FAF as

well as automated OCT segmentation of RPE loss and EZ loss on an example B-scan as well as on the en face images are provided in Fig. 1.

Statistical analysis

The areas of RPE loss and EZ loss measured automatically on OCT were compared to the hypofluorescent GA areas measured manually on FAF by the centralized reading center of the trials. Only images where the GA lesion was within the field of view on the baseline OCT were included in the cross-sectional analysis to be able to reliably compare the two imaging modalities in the assessment of GA measurements. The OCT-based RPE loss and EZ loss areas were calculated by multiplying the number of respectively segmented A-scans with the pixel area reported by the OCT device. The correlation between the areas in mm^2 measured on OCT vs. on FAF was reported using Pearson's correlation coefficient (r) and coefficient of determination (R^2) for baseline, month 12 and month 24 for both trials. Scatterplots were generated to compare the OCT- and FAF-derived GA area measurements. In addition, the mean difference was evaluated with Bland–Altman plots. The longitudinal correlation between the OCT-based RPE and FAF-based GA lesion growth over time was evaluated using the correlation for the change from baseline (CFB) GA lesion size using a square root transformation. Only eyes that had both OCT and FAF measurements at the analysis visits were included in this analysis. The CFB was calculated as the difference between the post-baseline GA lesion area and the GA lesion area at baseline. Descriptive statistics were produced with the absolute values for RPE loss on OCT and GA lesion size on FAF at each analysis visit. A mixed model for repeated measures (MMRM) adjusting for baseline RPE loss on OCT and GA lesion size on FAF was produced for the analysis of change from baseline of RPE loss on OCT and GA lesion size on FAF, respectively.

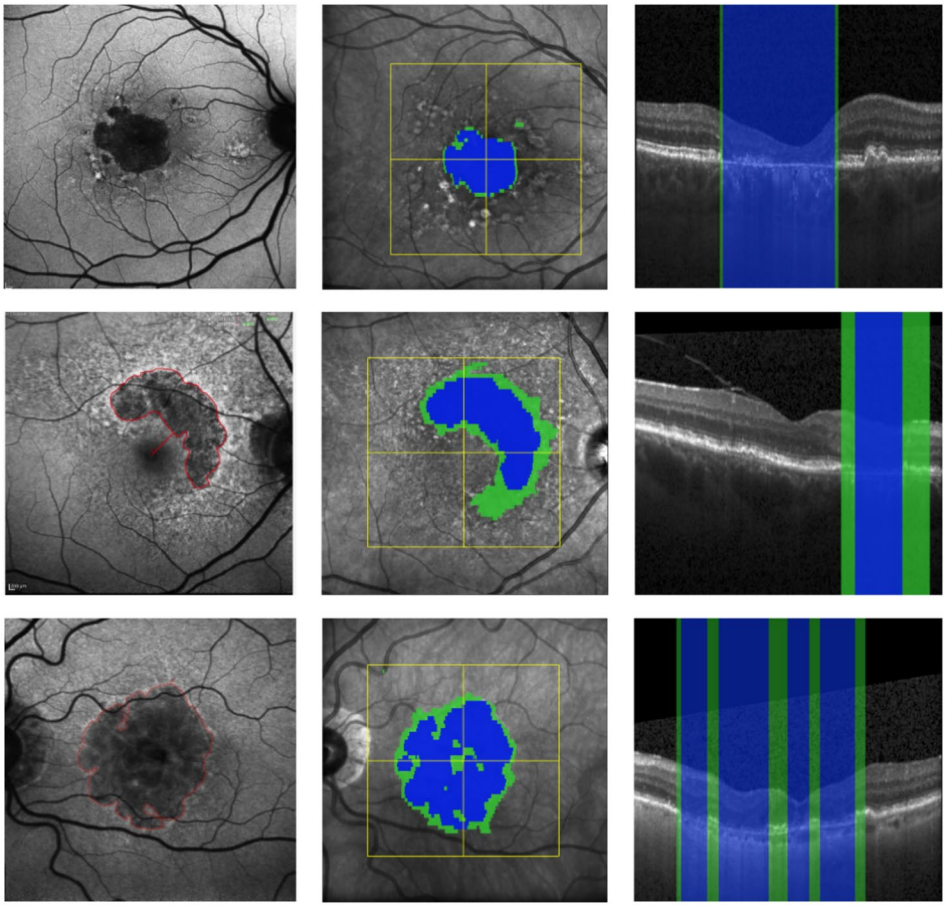

Fig. 1. Examples of manual GA segmentation on FAF (left column) and automated OCT segmentation of RPE loss (blue) and EZ loss (green) on the en face near-infrared reflectance image (middle column) and example B-scan (right column). The first row represents an example of strong correlation between RPE loss and EZ loss measurement on OCT compared to the GA measurement on FAF. The middle row represents an example of strong correlation between RPE loss and weak correlation of EZ loss on OCT compared to the GA measurement on FAF because of a high EZ/RPE loss ratio. The last row represents an example of weak correlation for both RPE loss and EZ loss on OCT compared to the GA measurement on FAF. Note how the assessment of foveal involvement differs between FAF and OCT evaluation.

Results

Study population

In total, 1258 patients were included in the OAKS and DERBY trials. In OAKS and DERBY 637 and 621 patients were included and 436 and 433 study eyes were imaged with a Spectralis OCT, respectively. Patients in which the GA lesion expanded over the field of view on OCT were excluded from the cross-sectional analysis, resulting in 365 and 354 patients at baseline, 305 and 282 patients at month 12 and 279 and 269 patients at month 24 from the OAKS and DERBY trials, respectively. Mean age was 78.0 ± 7.24 and 78.5 ± 7.06 years and 61.0% and 60.7% were of female gender in the OAKS and DERBY trials, respectively.

Correlation between manual FAF-based GA area and automated OCT-based RPE loss

In OAKS, mean GA lesion measured on FAF was 7.90 ± 3.75 mm^2 and RPE loss measured on OCT was 6.84 ± 3.17 mm^2 at baseline, 9.66 ± 4.25 mm^2 on FAF and 8.20 ± 3.50 mm^2 on OCT at month 12 and 11.24 ± 4.67 mm^2 on FAF and 9.29 ± 3.62 mm^2 on OCT at month 24. In DERBY, the mean GA lesion measured on FAF was 7.89 ± 3.92 mm^2 and RPE loss measured on OCT was 6.82 ± 3.36 mm^2 at baseline, 9.69 ± 4.24 mm^2 on FAF and 8.12 ± 3.52 mm^2 on OCT at month 12 and 11.42 ± 4.67 mm^2 on FAF and 9.53 ± 3.88 mm^2 on OCT at month 24. The correlation between absolute GA measurements on FAF and RPE loss on OCT was high and consistent for all time points. There was a correlation coefficient of 0.97 (R^2 = 0.94) at baseline and at month 12 and 0.96 (R^2 = 0.92) at month 24 in OAKS. In DERBY, the correlation coefficient between GA measurement on FAF and RPE loss on OCT was 0.97 (R^2 = 0.93) at baseline, 0.96 (R^2 = 0.92) at month 12 and 0.96 (R^2 = 0.91) at month 24 (Fig. 2). The mean difference in GA measurements assessed by the Bland–Altman plots between the two imaging modalities was 0.93 ± 0.99 mm^2 at baseline, 1.11 ± 1.14 mm^2 at month 12 and 1.26 ± 1.24 mm^2 at month 24 in OAKS and 0.88 ± 1.03 mm^2 at baseline, 1.11 ± 1.21 mm^2 at month 12 and 1.16 ± 1.29 mm^2 at month 24 in DERBY. As the GA lesion progressed over time, the mean difference also slightly increased. The Bland–Altman plots showed a bias towards higher GA measurements assessed by FAF than by OCT, especially in larger lesions, both in OAKS and in DERBY (Fig. 2).

Correlation between manual FAF-based GA area and automated OCT-based EZ loss

In OAKS, the mean EZ loss measured on OCT was 10.60 ± 5.32 mm^2 at baseline, 11.38 ± 5.10 mm^2 at month 12 and 12.67 ± 5.26 mm^2 at month 24. In DERBY, the mean EZ loss was 10.83 ± 5.72 mm^2 at baseline, 11.83 ± 5.68 mm^2 at month 12 and 13.15 ± 5.93 mm^2 at month 24. The correlation between the absolute GA area measurements on FAF and the EZ loss measured on OCT was lower compared to the correlation of GA measurement on FAF to RPE loss on OCT with a correlation coefficient of 0.71 (R^2 = 0.50) at baseline, 0.79 (R^2 = 0.63) at month 12 and 0.75 (R^2 = 0.56) at month 24 in OAKS. In DERBY, the correlation coefficient between GA area measurement on FAF and EZ loss measured on OCT was 0.69 (R^2 = 0.47) at baseline, 0.69 (R^2 = 0.48) at month 12 and 0.75 (R^2 = 0.56) at month 24. The scatterplots in Fig. 3 show a consistently larger EZ loss area measured on OCT than the GA area measurements on FAF, representing the RPE loss area. The mean difference in GA measurements on FAF and EZ loss measured on OCT, assessed by the Bland–Altman plots, was 2.8 ± 3.7 mm^2 at baseline, 2.03 ± 3.05 mm^2 at month 12 and 2.05 ± 3.38 mm^2 at month 24 in OAKS and 3.13 ± 4.16 mm^2 at baseline, 2.65 ± 4.13 mm^2 at month 12 and 2.41 ± 3.96 mm^2 at month 24 in DERBY. The Bland–Altman plots showed a bias towards higher EZ loss measurements on OCT than GA area assessed on FAF (Fig. 3).

Correlation for longitudinal change from baseline between manual FAF-based GA area and automated OCT-based RPE loss

At month 12, the abolute lesion growth was smaller on OCT compared to FAF by a mean difference of 0.18 ± 0.17 mm in the OAKS trial and by a mean of 0.18 ± 0.18 mm in the DERBY trial. At month 24, the absolute lesion growth was smaller on OCT compared to FAF by a mean difference of 0.19 ± 0.18 mm in the OAKS trial and 0.18 ± 0.18 mm in the DERBY trial. While CFB in GA lesion size measured on FAF and CFB of the area of RPE loss measured on OCT was weakly to moderately correlated at early timepoints, the CFB measured by FAF and OCT were highly correlated at later timepoints: r = 0.78 in OAKS and r = 0.74 in DERBY at month 12 and r = 0.89 in OAKS and r = 0.85 in DERBY at month 24. The correlation coefficient increased continually as the GA lesion areas and therefore the CFB increased (Fig. 4). When adjusting for baseline RPE loss on OCT and GA lesion size on FAF in the MMRM model, the mean CFB on OCT was slightly larger than on FAF (Fig. 5).

Discussion

Previous studies have been conducted to investigate the correlation between FAF and OCT for the measurement of GA lesions[11,18,19]. In the meantime, there has been a major breakthrough with the approval of novel therapies for GA. Under these circumstances, the correlation between the imaging modality used in clinical trials, i.e., FAF and the imaging modality used ubiquitously in clinical practice, i.e., OCT needs to be reassessed. In addition, fast and standardized approaches are in high demand to manage the increasing number of patients in clinics who require regular follow-up and treatment monitoring.

With this work, we investigated the correlation of manual reading center-based FAF measurements and automated OCT measurements of GA secondary to AMD in the two largest successful prospective phase 3 clinical OAKS and DERBY trials to date. The OCT volumes were analyzed by two previously validated complementary algorithms for RPE loss and EZ loss in GA lesions[15,16]. We showed that the correlation between manual GA area measurements on FAF and automated RPE loss measurements on OCT was high and consistent over time in both clinical trials. The correlation of the longitudinal CFB was weak to moderate at early time points. GA is a generally slowly progressive disease and therefore the CFB represents a very small region in the first few months, especially under treatment[20]. Over time, the correlation for the CFB increased as the GA lesions progressed and

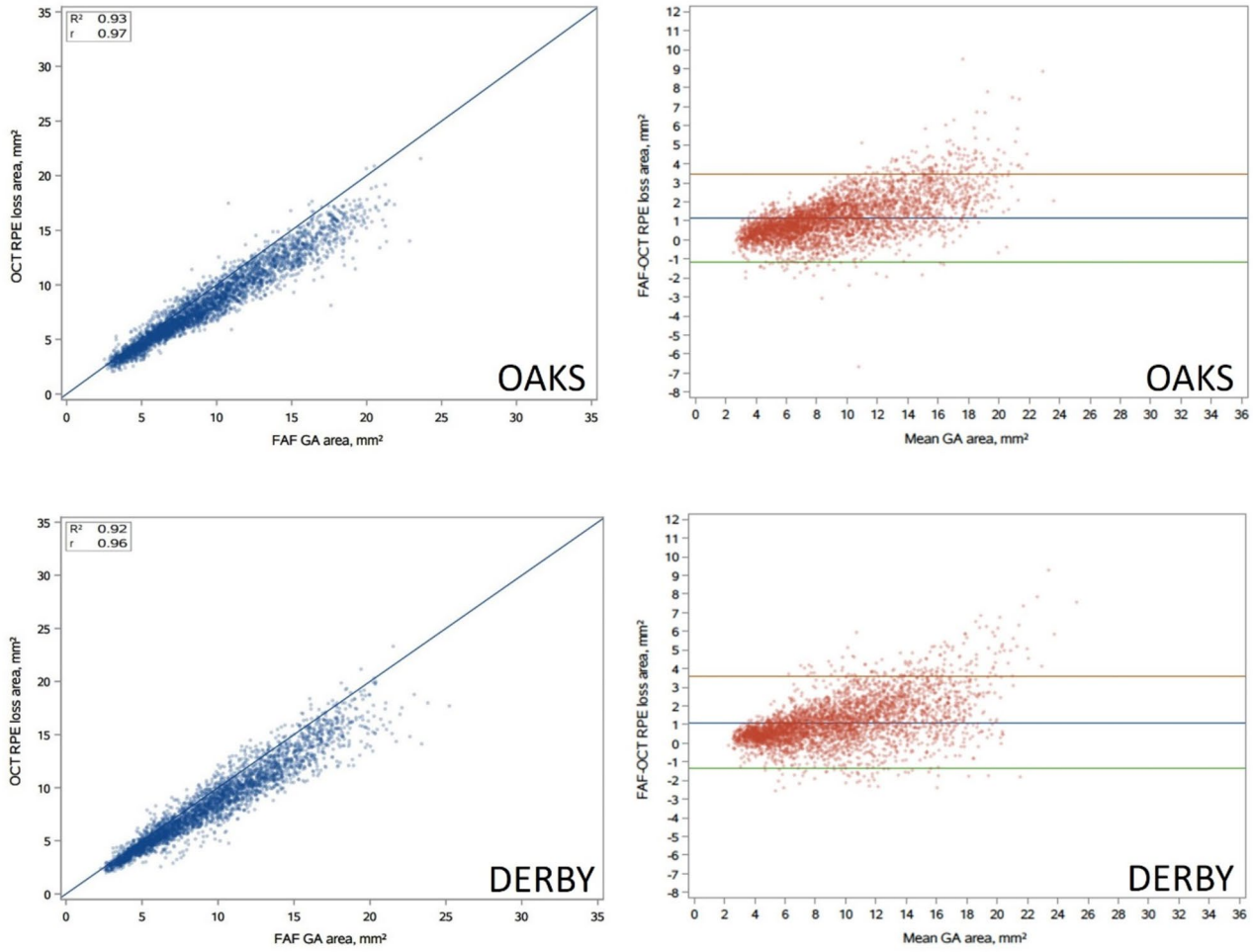

Fig. 2. Scatterplots (left) and Bland–Altman plots (right) between automated RPE loss measurement on OCT and manual GA measurement on FAF for OAKS (first row) and DERBY (second row) for all timepoints pooled. There was a high correlation between OCT and FAF measurements (r = 0.96) in both trials. The scatterplots and Bland–Altman plots show a bias towards slightly higher GA measurements on FAF compared to OCT, especially in larger lesions in both trials.

the correlation for the CFB was high at month 12 and 24 between the imaging modalities. We can therefore conclude that the overall correlation for the cross-sectional as well as the longitudinal assessment of GA progression is high between manual FAF and automated OCT measurements.

There was a bias of larger GA area measurements on FAF than RPE loss on OCT, which is in line with previous studies[11,21,22]. We and other groups hypothesize that OCT provides more precise differentiation between different stages of RPE attenuation, especially at the borders of GA, the junctional zone[11,22]. In addition, due to the difference in magnification between FAF and OCT, the pixel size in FAF images could be overestimated and therefore leading to a bias. Moreover, as shown in Fig. 1, there could be some cases where the fovea was graded as part of the atrophy on FAF while it was still preserved on OCT leading to higher atrophy measures on FAF. It has been shown previously that OCT is more precise and has a higher certainty for the evaluation of foveal sparing due to the presence of macular pigment at the fovea that blocks the blue excitation light on FAF imaging[11]. A pixelwise evaluation between co-registered OCT and FAF would be needed to comprehensively investigate the difference in retinal structures measured by the two imaging modalities. One study investigated co-registered FAF and OCT images and compared different FAF levels to outer retinal thickness measurements[23]. The study showed that the overall differences in mean RPE, PR layer and ONL thickness across FAF levels were statistically significant, highlighting the importance of a distinct assessment of retinal layers on OCT.

While blue-light FAF is still the gold standard imaging modality to asses GA lesion size and growth in clinical trials, more insights about the pathomechanisms and progression in GA have been gained by the advent of high-resolution 3D OCT imaging[9]. Moreover, regular OCT monitoring is recommended for patients receiving intravitreal injections with complement inhibitors to screen for signs of exudation because both approved treatments—pegcetacoplan as well as avacincaptad pegol—showed an increased risk of development of macular neovascularization in the clinical trials[3,5]. From comprehensive imaging and histopathological studies, we know that GA is characterized by a progressive loss of RPE, PR layers and decreased choriocapillaris perfusion[24,25]. Especially the photoreceptor layer is of interest since it has been shown that the PR integrity loss outside the

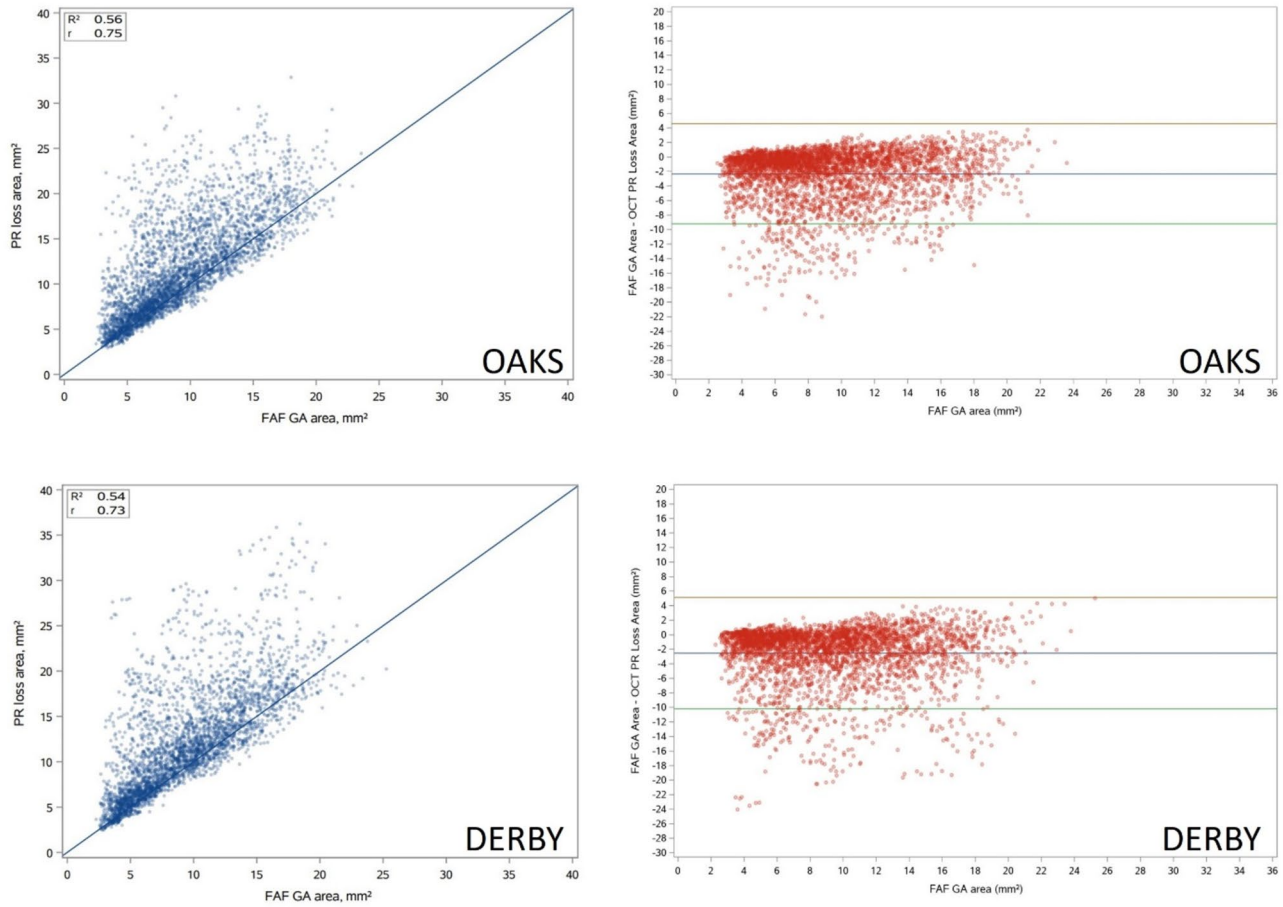

Fig. 3. Scatterplots (left) and Bland–Altman plots (right) between automated EZ loss measurement on OCT and manual GA measurement on FAF for OAKS (first row) and DERBY (second row) for all timepoints pooled. There was a high correlation in both trials with consistently larger EZ loss measurement on OCT compared to the GA measurement on FAF, representing the RPE loss.

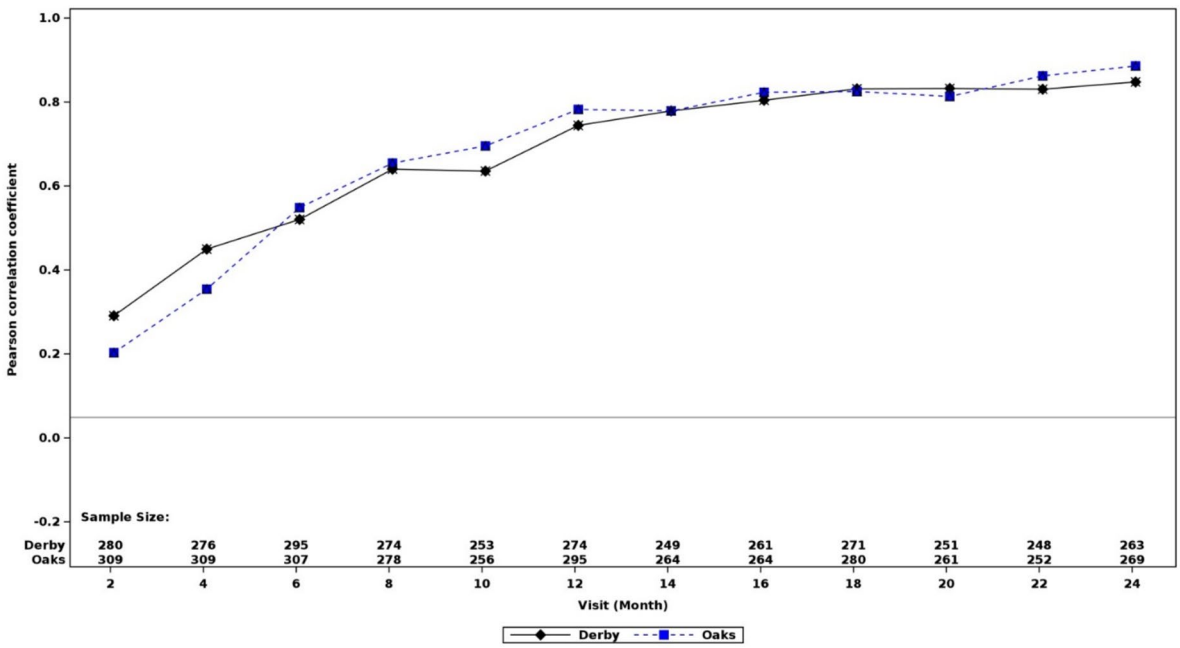

Fig. 4. Correlation coefficient for the longitudinal change from baseline (CFB) over time between automated RPE loss measurement on OCT and manual FAF measurement for GA. At early time points, the correlation was weak to moderate and increased over time, with a high correlation at later points in both trials.

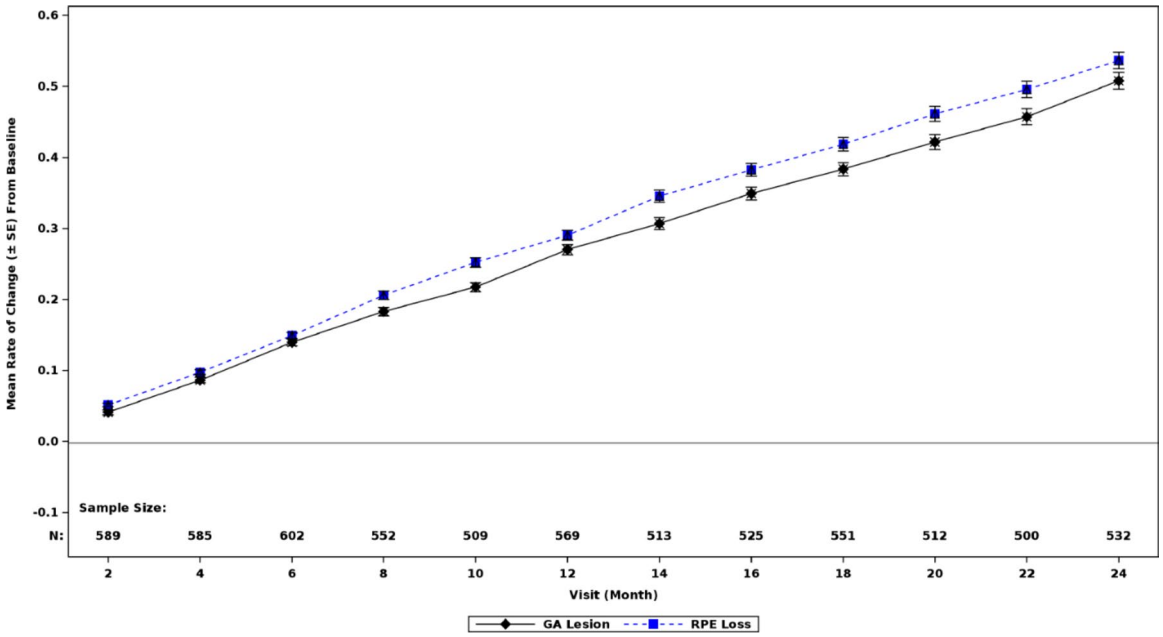

Fig. 5. Mean change from baseline for automated RPE loss on OCT (blue) and manual GA growth on FAF (black) with MMRM model. After adjusting for baseline RPE loss on OCT and GA lesion size on FAF in the MMRM model, the mean CFB on OCT was slightly larger than on FAF.

borders of the RPE loss is strongly correlated with GA progression[26,27]. However, the PR layer cannot be visualized reliably on FAF[19]. Therefore, 2D FAF does not provide information on the whole disease extent and activity in GA patients.

In our study, the correlation between PR integrity loss, defined as EZ loss, on OCT and GA measurements on FAF was lower than the correlation with RPE loss. The mean EZ loss measurements were consistently larger than the FAF measurements, representative of the RPE loss. This supports the general belief that EZ loss precedes the development of RPE loss[11,18,19,23]. However, this does not necessarily explain the weaker correlation of EZ loss to FAF measurements compared to the correlation of RPE loss to FAF measurements in our analysis. Previous work by our group has shown that there can be a substantial variability of alterations of the PR layer in the junctional zone, adjacent to the RPE loss area, which could explain the lower correlation and highlights the heterogeneity of morphologic disease presentation[13,28].

Other previous studies which investigated the correlation between FAF and OCT measurements in GA were limited in sample size and correlated manual segmentations on OCT and FAF. In a systematic comparison of FAF and OCT it was shown that decreased FAF correlated best to the choroidal signal enhancement on OCT[11]. Moreover, similar to our findings, the area of RPE loss on OCT was smaller than the GA size on FAF and the PR alterations were more extensive than complete RPE alterations. These findings were confirmed in a longitudinal comparison of GA progression on FAF and OCT[19]. However, these studies are not directly comparable to our study as they used different definitions for the PR layer. Another study on FAF and OCT comparison, that investigated the inner and outer segments of the PR layer, could show that the largest linear dimensions in GA were measured for the PR loss, followed by choroidal hyperreflectivity, FAF loss and RPE attenuation[18]. They also concluded that the PR integrity loss precedes complete RPE cell loss.

One recent study investigated the correlation between manual FAF and automated en face OCT measurements[22]. They used an instrument software of the Cirrus device to delineate the GA area on OCT at the level of the choroid. However, the segmentations needed manual corrections. After manual corrections, there was a high correlation between FAF and OCT measurements ($r = 0.98$) with a mean difference of 1.01 mm^2, which is in line with our results. The authors again explained this finding due to the variability of the RPE and preserved PR at the GA border[22]. We believe that software algorithms for GA segmentation should therefore be based on complete segmentation of retinal compartments and layers instead of choroidal hypertransmission, which ignores morphologic alterations, to be able to precisely determine disease activity and therapeutic efficacy.

PR integrity loss, measured as EZ loss, in particular is associated with future GA growth, both globally and locally[26]. In post-hoc analyses of the phase 2 FILLY trial as well as the phase 3 OAKS and DERBY trials we showed that the treatment effect of pegcetacoplan is even more pronounced on the EZ layer maintenance[13,28]. As the PR layer is the correlate of visual function, it will be indispensable to accurately monitor the PR status in GA patients, especially under therapeutic conditions, highlighting the importance of automated OCT-based monitoring of EZ loss in GA patients[29–32]. This has also been underlined by the recent acknowledgment of EZ loss as an outcome measurement in GA trials by the FDA[33].

In previous works we described the EZ/RPE loss ratio as an important biomarker for different phenotypes of disease activity in GA. We showed in post-hoc analyses that patients with a high EZ/RPE loss ratio had a faster

progression and a better therapeutic efficacy in the phase 2 FILLY trial and the phase 3 OAKS and DERBY trials of pegcetacoplan[13,28].

Limitations of our analysis include a possible selection bias due to the post-hoc analysis of a potential non-random subset from the OAKS and DERBY trials. Furthermore, this also defines the minimal GA size and the type of the FAF signal defined by the inclusion criteria of the trial (lesions > 2.5 mm^2). Moreover, as the primary clinical trials were planned with regard to FAF measurements, the data was not statistically predetermined for OCT-based analysis. We controlled for RPE loss relative to the OCT imaging field but were not able to control for the corresponding EZ loss as it was not visible on FAF. Only patients that were imaged with a Spectralis device were included in this analysis due to the higher image quality because of the signal to noise ratio. Further analyses are needed to evaluate the correlation of automated GA measurement on different OCT devices to conventional FAF assessment.

In summary, we conclude that OCT is well suited to monitor disease activity and progression in GA patients in clinical practice. In addition to the RPE layer, the PR status, represented by the EZ layer, can be assessed precisely with AI-based analysis on OCT, which offers more insight into pathomorphologic changes and treatment effects. With this work, we showed that automated OCT analysis is consistent for GA measurements compared to manual FAF during complement inhibitory treatment in two large prospective clinical trials. We believe that automated and objective AI methods on OCT will offer a paradigm shift and guidance for GA management in clinical practice. AI-based GA monitoring can be used for future clinical trials to offer objective and reproducible results as well as in routine clinical practice to provide fast and automated quantifications of GA lesions on OCT.

Data availability

Original data for this research were provided by Apellis Pharmaceuticals. Data that support the findings of this study are available upon reasonable request from the corresponding author.

Received: 4 June 2024; Accepted: 28 August 2024
Published online: 04 September 2024

References

1. Apellis. *FDA Approves SYFOVRE™ (pegcetacoplan injection) as the First and Only Treatment for Geographic Atrophy (GA), a Leading Cause of Blindness*. https://investors.apellis.com/news-releases/news-release-details/fda-approves-syfovretm-pegcetacoplan-injection-first-and-only (2023).
2. Liao, D. S. *et al.* Complement C3 inhibitor pegcetacoplan for geographic atrophy secondary to age-related macular degeneration: A randomized phase 2 trial. *Ophthalmology* **127**, 186–195. https://doi.org/10.1016/j.ophtha.2019.07.011 (2020).
3. Heier, J. S. *et al.* Pegcetacoplan for the treatment of geographic atrophy secondary to age-related macular degeneration (OAKS and DERBY): Two multicentre, randomised, double-masked, sham-controlled, phase 3 trials. *Lancet* **402**, 1434–1448. https://doi.org/10.1016/s0140-6736(23)01520-9 (2023).
4. Astellas. Iveric Bio Receives U.S. FDA Approval for IZERVAY™ (avacincaptad pegol intravitreal solution), a New Treatment for Geographic Atrophy (2023).
5. Khanani, A. M. *et al.* Efficacy and safety of avacincaptad pegol in patients with geographic atrophy (GATHER2): 12-month results from a randomised, double-masked, phase 3 trial. *Lancet* https://doi.org/10.1016/s0140-6736(23)01583-0 (2023).
6. Göbel, A. P., Fleckenstein, M., Schmitz-Valckenberg, S., Brinkmann, C. K. & Holz, F. G. Imaging geographic atrophy in age-related macular degeneration. *Ophthalmologica* **226**, 182–190. https://doi.org/10.1159/000330420 (2011).
7. Boyer, D. S., Schmidt-Erfurth, U., van Lookeren Campagne, M., Henry, E. C. & Brittain, C. The pathophysiology of geographic atrophy secondary to age-related macular degeneration and the complement pathway as a therapeutic target. *Retina* **37**, 819–835. https://doi.org/10.1097/iae.0000000000001392 (2017).
8. Fleckenstein, M. *et al.* The progression of geographic atrophy secondary to age-related macular degeneration. *Ophthalmology* **125**, 369–390. https://doi.org/10.1016/j.ophtha.2017.08.038 (2018).
9. Cleland, S. C. *et al.* Quantification of geographic atrophy using spectral domain OCT in age-related macular degeneration. *Ophthalmol. Retina* **5**, 41–48. https://doi.org/10.1016/j.oret.2020.07.006 (2021).
10. Schmidt-Erfurth, U., Klimscha, S., Waldstein, S. M. & Bogunović, H. A view of the current and future role of optical coherence tomography in the management of age-related macular degeneration. *Eye (Lond)* **31**, 26–44. https://doi.org/10.1038/eye.2016.227 (2017).
11. Sayegh, R. G. *et al.* A systematic comparison of spectral-domain optical coherence tomography and fundus autofluorescence in patients with geographic atrophy. *Ophthalmology* **118**, 1844–1851. https://doi.org/10.1016/j.ophtha.2011.01.043 (2011).
12. Schmidt-Erfurth, U., Sadeghipour, A., Gerendas, B. S., Waldstein, S. M. & Bogunović, H. Artificial intelligence in retina. *Prog. Retin. Eye Res.* **67**, 1–29. https://doi.org/10.1016/j.preteyeres.2018.07.004 (2018).
13. Riedl, S. *et al.* The effect of pegcetacoplan treatment on photoreceptor maintenance in geographic atrophy monitored by artificial intelligence-based OCT analysis. *Ophthalmol. Retina* **6**, 1009–1018. https://doi.org/10.1016/j.oret.2022.05.030 (2022).
14. Vogl, W. D. *et al.* Predicting topographic disease progression and treatment response of pegcetacoplan in geographic atrophy quantified by deep learning. *Ophthalmol. Retina* https://doi.org/10.1016/j.oret.2022.08.003 (2022).
15. Lachinov, D., Seeböck, P., Mai, J., Schmidt-Erfurth, U. & Bogunović, H. *Projective Skip-Connections for Segmentation Along a Subset of Dimensions in Retinal OCT* (2021).
16. Orlando, J. I. *et al.* Automated quantification of photoreceptor alteration in macular disease using optical coherence tomography and deep learning. *Sci. Rep.* **10**, 5619. https://doi.org/10.1038/s41598-020-62329-9 (2020).
17. Mai, J. *et al.* Clinical validation for automated geographic atrophy monitoring on OCT under complement inhibitory treatment. *Sci. Rep.* **13**, 7028. https://doi.org/10.1038/s41598-023-34139-2 (2023).
18. Schmitz-Valckenberg, S., Fleckenstein, M., Göbel, A. P., Hohman, T. C. & Holz, F. G. Optical coherence tomography and autofluorescence findings in areas with geographic atrophy due to age-related macular degeneration. *Investig. Ophthalmol. Vis. Sci.* **52**, 1–6. https://doi.org/10.1167/iovs.10-5619 (2011).
19. Simader, C. *et al.* A longitudinal comparison of spectral-domain optical coherence tomography and fundus autofluorescence in geographic atrophy. *Am. J. Ophthalmol.* **158**, 557-566.e551. https://doi.org/10.1016/j.ajo.2014.05.026 (2014).
20. Shen, L., Liu, F., Grossetta Nardini, H. & Del Priore, L. V. Natural history of geographic atrophy in untreated eyes with nonexudative age-related macular degeneration: A systematic review and meta-analysis. *Ophthalmol. Retina* **2**, 914–921. https://doi.org/10.1016/j.oret.2018.01.019 (2018).

21. Mai, J. *et al.* Comparison of fundus autofluorescence versus optical coherence tomography-based evaluation of the therapeutic response to pegcetacoplan in geographic atrophy. *Am. J. Ophthalmol.* **244**, 175–182. https://doi.org/10.1016/j.ajo.2022.06.023 (2022).
22. Velaga, S. B., Nittala, M. G., Hariri, A. & Sadda, S. R. Correlation between fundus autofluorescence and en face OCT measurements of geographic atrophy. *Ophthalmol. Retina* **6**, 676–683. https://doi.org/10.1016/j.oret.2022.03.017 (2022).
23. Wang, D. L. *et al.* Outer retinal thickness and fundus autofluorescence in geographic atrophy. *Ophthalmol. Retina* **3**, 1035–1044. https://doi.org/10.1016/j.oret.2019.07.016 (2019).
24. Li, M. *et al.* Histology of geographic atrophy secondary to age-related macular degeneration: A multilayer approach. *Retina* **38**, 1937–1953. https://doi.org/10.1097/iae.0000000000002182 (2018).
25. Li, M. *et al.* Clinicopathologic correlation of geographic atrophy secondary to age-related macular degeneration. *Retina* **39**, 802–816. https://doi.org/10.1097/iae.0000000000002461 (2019).
26. Reiter, G. S. *et al.* Subretinal drusenoid deposits and photoreceptor loss detecting global and local progression of geographic atrophy by SD-OCT imaging. *Investig. Ophthalmol. Vis. Sci.* **61**, 11. https://doi.org/10.1167/iovs.61.6.11 (2020).
27. Lindner, M. *et al.* Local progression kinetics of geographic atrophy in age-related macular degeneration are associated with atrophy border morphology. *Investig. Ophthalmol. Vis. Sci.* **59**, Amd12-amd18. https://doi.org/10.1167/iovs.17-23203 (2018).
28. Schmidt-Erfurth, U. *et al.* Therapeutic effect of pegcetacoplan on retinal pigment epithelium (RPE) and photoreceptor (PR) integrity in geographic atrophy (GA) in the phase III OAKS and DERBY trials. *Investig. Ophthalmol. Vis. Sci.* **64**, 919–919 (2023).
29. Takahashi, A. *et al.* Photoreceptor damage and reduction of retinal sensitivity surrounding geographic atrophy in age-related macular degeneration. *Am. J. Ophthalmol.* **168**, 260–268. https://doi.org/10.1016/j.ajo.2016.06.006 (2016).
30. Pilotto, E. *et al.* Microperimetry, fundus autofluorescence, and retinal layer changes in progressing geographic atrophy. *Can. J. Ophthalmol.* **48**, 386–393. https://doi.org/10.1016/j.jcjo.2013.03.022 (2013).
31. Hariri, A. H., Tepelus, T. C., Akil, H., Nittala, M. G. & Sadda, S. R. Retinal sensitivity at the junctional zone of eyes with geographic atrophy due to age-related macular degeneration. *Am. J. Ophthalmol.* **168**, 122–128. https://doi.org/10.1016/j.ajo.2016.05.007 (2016).
32. Sayegh, R. G. *et al.* A systematic correlation of morphology and function using spectral domain optical coherence tomography and microperimetry in patients with geographic atrophy. *Br. J. Ophthalmol.* **98**, 1050–1055. https://doi.org/10.1136/bjophthalmol-2014-305195 (2014).
33. Stealth, B. *StealthBio Therapeutics Announces Positive End-of-Phase 2 Meeting with FDA on the Development of Elamipretide in Patients with Dry Age-related Macular Degeneration*. https://www.prnewswire.com/news-releases/stealth-biotherapeutics-announces-positive-end-of-phase-2-meeting-with-fda-on-the-development-of-elamipretide-in-patients-with-dry-age-related-macular-degeneration-301848690.html (2023).

Author contributions

JM, GRS, SR, HB, USE: conception and design of the study. EF, AM, WDV, AS: data collection and analysis. JM, GRS, SR, HB, USE: interpretation of the data. JM: preparation of manuscript. All authors were responsible for critical revision of the manuscript and final approval of the manuscript.

Funding

This work was financially supported by an Apellis research grant as part of the contract research to the Medical University of Vienna.

Competing interests

The OAKS and DERBY trials were conducted by Apellis Pharmaceuticals and our work was in part supported by an Apellis research grant. Financial Disclosures: Julia Mai: Consultancy: Apellis, Roche Gregor S. Reiter: Contract Research: RetInSight, Consultancy: Apellis, Bayer, Roche Sophie Riedl: No financial disclosures Wolf-Dieter Vogl: Employment RetInSight Amir Sadeghipour: Employment RetInSight Emma Foos: Employment Apellis Alex McKeown: Employment Apellis Hrvoje Bogunovic: Contract Research to the Medical University of Vienna: Apellis, Heidelberg Engineering Ursula Schmidt-Erfurth: Scientific Consultant: Apellis, Aviceda, Complementtherapeutix, Heidelberg Engineering, Novartis, ONL, RetInSight, Roche, Topcon Contract Research to the Medical University of Vienna: Apellis, Genentech, Kodiak.

Additional information

Correspondence and requests for materials should be addressed to U.S.-E.